Material Transport from Nonspherical Particles

S. N. Upadhyay, M. Singh,* P. N. Dwivedi,[1] and G. Tripathi
Department of Chemical Engineering, Institute of Technology, Banaras Hindu University, Varanasi 221005, India

Forced convective mass transfer between a solid nonspherical particle and water was studied for $0.1993 < (D_p/D_c) < 0.477$ and $50 < N_{Rec} < 25000$. No effect of (D_p/D_c) was observed in the range studied. The experimental results were correlated by $N_{Sh}N_{Sc}^{-1/3} = 0.5844 N_{Rec}^{1/2} + 0.006012 N_{Rec}$.

Mass (or heat) transfer between particles surrounded by a continuous fluid phase is of importance in many engineering operations. Typical examples include absorption, adsorption, aerodynamics, bubble plate distillation column, calcining, catalytic beds, desorption, drying, liquid-liquid and solid-liquid extraction, leaching, nuclear reactors, and spray drying. Although most of these operations involve multiparticle systems, due to simplicity, transfer from single spheres, droplets, etc., has received much attention.

Transfer of mass (or heat) between a particle and a surrounding fluid phase can occur by three mechanisms: diffusion (or conduction), natural convection, and forced convection. These mechanisms may act individually or collectively. The actual nature of the combination and interaction of individual mechanisms is still largely unresolved; however, their role may be described by the conventional dimensionless groups used to correlate the overall mass (or heat) transfer rates, i.e., by

$$N_{Sh} \text{ (or } N_{Nu}) = f[N_{Re}, N_{Sc} \text{ (or } N_{Pr}), N_{Gr}] \quad (1)$$

Pure diffusion (or conduction) can occur when N_{Re} and N_{Gr} both are zero. This condition is realized by suspending the particle in a stagnant fluid; however, such a condition is difficult to realize in practice.

Natural convection occurs when $N_{Gr} > 0$. In this case, the transfer results from the flow of the surrounding fluid, which is promoted by differences in the fluid density which, in turn, are due to concentration and/or temperature gradients.

Forced convection comes into the picture when $N_{Re} > 0$, i.e., when a relative flow exists between the fluid and the particle.

Considerable theoretical and experimental information on the forced convective mass (or heat) transfer from single particles to a surrounding fluid exists in the literature, and many excellent reviews on the subject are available (*9–11, 15, 17, 31, 35*). Most of the earlier studies have been aimed at establishing the exact nature of Equation 1 by analyzing or measuring the rate of mass (or heat) between the particle and air or water. The most widely studied particle shape is spherical; little information is available for other shapes.

The present work is aimed at obtaining the mass transfer rate data for particles of shapes other than spherical. For this purpose, the rates of dissolution of cylindrical and modified cylindrical pellets of benzoic acid in water are measured in the range $50 < N_{Rec} < 25000$. The results are correlated in terms of the Sherwood and Reynolds numbers and are compared with the previous published data on spheres.

[1] Present address, Department of Mechanical Engineering, Institute of Technology, Banaras Hindu University, Varanasi 221005, India.

Experimental

The test fluid in all runs was tap water because of its abundant availability. Cylindrical and modified cylindrical pellets were prepared as described elsewhere (*41*). The diameter and thickness measurements were made on 50 randomly chosen samples from each pellet size with the help of a micrometer. The arithmetic average of these was used to calculate the surface area, equivalent particle diameter, and volume of the pellets.

The pellets were fixed at the end of 10-cm long 1-mm diam stainless-steel wires which served as support rods. One end of the wire was heated just above the melting point of benzoic acid and was embedded radially in the pellet. The radical position of the wire was carefully maintained by means of an aligner until its end was firmly held by the solidification of the molten acid. The length of the wire inside the pellets was of the order of 2–3 mm. The embedded wires did not come out easily. Any molten material sticking to the wire surface was removed with the help of a fine file, and the particle surface was polished with tissue paper. Each prepared pellet was rewashed and dried to a constant weight in a desiccator before being used for the actual run.

Except for a few minor alterations in the test section, the experimental setup was essentially the same as used earlier (*41*). Water from a constant head storage tank was pumped and metered through the rotameters to the test column. A bypass provided at the discharge side of the pump facilitated better flow control. A thermometer capable of reading up to $^1/_{10}$ of a degree centigrade indicated the water temperature at the inlet end of the column. After flowing past the test particle in the column, water was discharged through a ditching line. Another thermometer capable of reading up to $^1/_{10}$ of a degree centigrade and installed at the exit end of the column indicated the temperature of the outgoing stream. Three different test columns of i.d. 2.35, 2.97, and 5.71 cm were used. Each was about a 100-cm long pyrex glass tube. The details of the test columns are shown in Figure 1. The particle mounting device was made of a 0.6-cm diameter stainless-steel rod which was about 32 cm long. The particle support wire was attached to this rod through a brass holder, and the whole assembly, in turn, was suspended in the test column through a standard Quickfit brass gland. By means of two tightening screws, one in the particle suspension rod and the other in the brass gland, it was possible to adjust the position of the pellet in the center of the column.

The water level in the test column was adjusted below the particle position. A test particle weighed to the nearest 0.05 mg was mounted in it, and the flow was started. A stop watch was started when the particle was half dipped in the rising level of water in the test column. Any air bubble sticking to the particle surface was removed by gently tapping the particle mounting rod. Depending upon the flow rate, the runs lasted for a period of 10–30 min. Flow rate and temperature at the inlet and outlet ends of the test column were frequently noted during the course of the run, and the arithmetic mean of these readings was used in the calculations. At the end of the desired period, the water circulation was stopped, and the test particle was taken out of the column, dried in a desiccator to a constant weight, and reweighed. The weight loss

so obtained was used to calculate the mass transfer rate. The evaporation loss during the drying was negligible; hence, no correction was considered necessary.

The mass transfer coefficients were calculated from the measured weight loss and the time of run by

$$k_c' = \frac{\Delta W}{A_p t(C_s - C_b)} \tag{2}$$

The fluid velocities based on the empty column cross section were converted to the Reynolds number using the equivalent particle diameter based on the surface area as the characteristic length parameter and the kinematic viscosity of water at the temperature of the measurement. The mass transfer coefficients were converted to the Sherwood number using the equivalent particle diameter as the characteristic length parameter and diffusivity of the solute in water at the temperature concerned. The solubility data for benzoic acid were taken from the literature (*5, 33, 34, 36, 38*). The diffusivities were calculated using Wilke and Chang's relation (*44*). The viscosity data of water were taken from Perry's handbook (*27*).

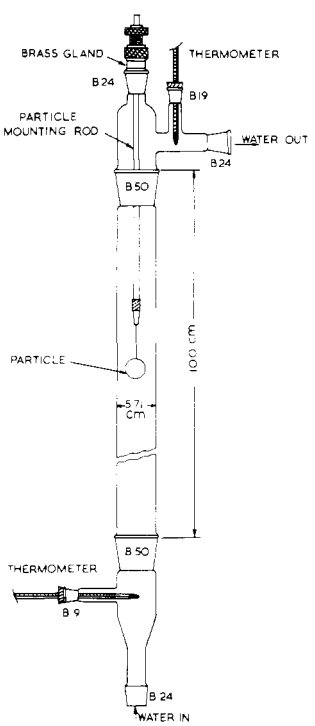

Figure 1. Test column

Table I. Range of Present Observations

Variable	Range
Particle diameter, D_p, cm	0.5961–1.1380
Particle shape	Cylindrical and modified cylindrical pellets
Column diameter, D_c, cm	2.35, 2.97, 5.71
Temperature, °C	16.2–29.6
Time of run, min	10.0–30.0
D_p/D_c	0.1993–0.4770
u, cm/sec	0.4910–170.8
k_c', cm/sec	0.000630–0.02022
N_{Sh}	107.7–2,298
N_{Sc}	759.0–1726
N_{Re}	54.0–21,200

The range of values of the different parameters covered in the present study is given in Table I, and typical data are listed in Table II.

Results and Discussion

Variation of the mass transfer coefficient, k_c', with the $N_{Re\infty}$, is shown in Figure 2. The data fall on separate and nearly parallel lines for each particle size, and the mass transfer coefficient increases with decreasing particle size.

The $N_{Sh}N_{Sc}^{-1/3}$ vs. Reynolds number, $N_{Re\infty}$, plots for all the particle sizes studied are shown in Figure 3. Experimental values for the various shapes and sizes fall on the same line, and no effect of the (D_p/D_c) ratio, which varied from 0.1993 to 0.477, is evident. The absence of the effect of the (D_p/D_c) ratio is clearer from Figure 4, which compares the present data with those of Rowe et al. (*31*) (D_p/D_c = 0.1666 to 0.400) and Tripathi et al. (*40*) (D_p/D_c = 0.2777 to 0.5660) for spheres.

For mass (or heat) transfer measurements being performed in closed conduits of limited size, Brown et al. (*1*), Vliet and Leppert (*42*), Robinson et al. (*30*), and Pope (*28*) have suggested the use of a velocity corrected for the blockage ratio. Pei (*26*) has shown that the correction factor

$$\frac{u_c}{u_\infty} = C_f = 1/[1 - \tfrac{2}{3}(d_s/D_c)^2] \tag{3}$$

used by Brown et al. (*1*) and Vliet and Leppert (*42*) gives the best correlation. In Figure 5 $N_{Sh}N_{Sc}^{-1/3}$ values for all particle sizes are plotted against the Reynolds number, N_{Rec}, corrected for the blockage effect. The use of the blockage ratio correction term only marginally improves the scattering of the data points. Similar behavior is evident from Figure 6 which compares the present results with those of Rowe et al. (*31*) and Tripathi et al. (*40*).

From Figures 4 and 6, it is also clear that the data for small nonspherical particles can be correlated along with those for spheres using a suitable form of correlating equation.

In deciding the exact nature of Equation 1 for correlating the forced convective mass transfer data for immersed spheres, one must know the influence of N_{Sc} and N_{Re} on the Sherwood number. Colburn (*3*) proposed that

$$N_{Sh} \alpha N_{Sc}^{1/3} \tag{4}$$

and this has been accepted and verified by many subsequent workers (*6–8, 12–14, 29*). Ruckenstein (*32*) pointed out that the Schmidt group exponent is a function of the magnitude of the Schmidt group of the system and recent work by many workers (*16, 18, 20, 21*) has shown that it may vary from 0.15 to 0.33. However, Equation 4 is still the most favored form of relation between the Sherwood and Schmidt numbers and has been assumed to be true for the present case also. For deciding the influence of the Reynolds number, the contribution to transfer is assumed to be made up of two components, one corresponding to the laminar boundary layer over the front portion and the other to the region of separation in the wake. Using Prandtl's boundary layer theory and neglecting the compressibility of the surrounding fluid and gravitational effects, Fröessling (*6–8*) showed that for nonangular bodies of revolution, the forward part Sherwood number is directly proportional to the square root of the Reynolds number. Most subsequent workers have used this approach in correlating their results and have used a relation of the form

$$N_{Sh} = A + BN_{Re}^{1/2}N_{Sc}^{1/3} \tag{5}$$

Many workers (*6–8, 14, 17, 19, 25, 29, 31*) have assigned a value of 2 to A, assuming it to be purely a contribution from the molecular diffusion (*16, 23, 29*). Steinberg and Treybal

Table II. Experimental Data

Run no. 1	T, °C 2	N_{Re} 3	N_{Rec} 4	$N \times 10^5$, g/cm²·s 5	$k_c^* \times 10^4$, cm/sec 6	N_{Sh} 7	$N_{Sh}N_{Sc}^{-1/3}$ 8
	D_p = 1.121 cm, A_p = 3.940 cm², V_p = 0.4296 cm³, D_c = 2.35 cm, D_p/D_c = 0.477, C_f = 1.083						
I-1	28.4	398.5	464.0	0.8460	22.03	464.0	24.62
I-4	28.4	1183	1380	0.9613	25.50	274.8	28.89
I-5	28.6	1585	1846	1.1474	30.18	321.8	33.90
I-6	28.5	1975	2300	1.2502	33.07	356.5	37.50
I-7	28.7	2380	2762	1.4598	38.30	408.0	43.05
I-8	28.8	2779	3235	1.6952	44.42	474.0	50.02
I-9	28.9	3188	3715	1.8295	47.63	503.0	53.15
I-10	29.0	3588	4175	1.9644	51.07	540.0	56.54
I-11	29.3	4010	4660	2.2482	58.22	609.0	64.54
I-12	25.4	5520	6435	2.3582	67.25	805.0	81.81
I-13	25.3	7350	8560	3.1069	88.70	1061	107.6
I-16	25.3	9180	10700	3.6695	105.0	1258	127.6
I-17	25.4	11050	12880	4.0100	138.7	1365	138.7
I-18	25.5	12910	15050	4.4965	127.5	1520	154.6
I-19	25.5	14780	17220	4.9026	138.8	1655	168.4
I-20	25.5	16610	19400	5.2664	149.2	1818	184.9
I-21	25.7	18520	21600	5.9981	168.9	2030	207.1
I-22	25.6	20400	23750	6.3915	180.9	2155	219.6
I-23	25.6	21200	24700	6.8124	192.5	2298	234.2
	D_p = 0.8973 cm, A_p = 2.529 cm², V_p = 0.2604 cm³, D_c = 2.35 cm, D_p/D_c = 0.3818, C_f = 1.066						
I-24	28.7	317.8	338.8	0.6063	15.92	136.1	14.35
I-25	28.7	635.6	679.0	0.6887	18.07	154.3	16.28
I-26	28.9	956.6	1020	0.9157	23.73	201.0	21.21
I-27	29.0	1278	1362	1.1053	28.51	241.5	25.55
I-28	28.4	1895	2020	1.2933	34.31	296.1	31.13
I-29	28.5	2216	2365	1.6004	42.34	365.0	38.40
I-30	28.6	2535	2705	1.9457	51.36	443.0	46.62
I-31	28.6	3174	3385	2.1187	55.76	477.0	50.25
I-32	26.0	4495	4785	2.1879	61.00	573.0	58.70
I-33	26.4	6035	6440	2.9767	81.80	757.0	77.94
I-34	26.3	7530	8040	3.4795	96.00	894.0	91.91
I-35	26.3	8930	9530	4.3461	119.8	1120	115.2
I-36	25.8	11910	12700	5.0677	141.9	1340	136.9
I-38	24.5	14500	15460	5.1699	151.5	1501	150.6
I-39	26.3	16600	17700	6.8470	188.5	1753	180.3
I-40	26.3	17310	18480	7.3347	202.0	1885	193.8
	D_p = 0.8569 cm, A_p = 2.200 cm², V_p = 0.2412 cm³, D_c = 2.35 cm, D_p/D_c = 0.3464, C_f = 1.07						
I-41	26.7	291.0	311.5	0.5443	12.31	107.7	11.13
I-44	30.0	1250	1338	1.1504	28.08	218.8	23.33
I-45	26.9	1462	1567	1.3315	36.00	311.5	32.27
I-46	26.1	1722	1842	1.4584	40.50	362.5	37.16
I-49	29.0	2748	2940	2.5228	63.90	517.0	54.64
I-50	29.0	3050	3265	1.9887	56.40	407.0	43.01
I-51	23.7	4075	4360	1.9698	59.30	577.0	57.14
I-52	24.8	5570	5960	2.7463	79.60	744.0	74.91
I-53	25.0	6990	7480	3.5721	103.0	956.0	96.58
I-54	25.1	8400	8980	4.0569	117.0	1085	109.8
I-55	25.2	9840	10530	4.5517	130.8	1212	122.8
I-56	25.2	11230	12000	4.7524	136.5	1260	127.7
I-57	25.2	12620	13500	4.9835	146.2	1322	134.0
I-58	25.2	14010	15000	5.3941	155.2	1434	145.3
I-59	25.2	15470	16500	5.3449	153.7	1428	154.0
I-60	25.2	16180	17300	6.2237	179.0	1652	167.4
	D_p = 0.8015 cm, A_p = 2.017 cm², V_p = 0.1962 cm³, D_c = 2.35 cm, D_p/D_c = 0.3411, C_f = 1.058						
I-69	28.7	2555	2700	2.3730	62.27	475.0	50.00
I-7028	28.8	2846	3010	2.5494	66.56	507.5	53.57
I-71	26.1	4020	4260	2.7742	76.50	640.0	65.61
I-73	26.3	6720	7115	3.8510	105.2	875.0	89.97
I-74	26.2	8050	8515	4.3386	121.0	1002	102.8
I-7526	26.1	9400	9840	4.8634	135.0	1130	115.8
I-76	25.9	12000	12700	6.0369	169.1	1420	145.2
I-79	25.8	14650	15500	6.9046	194.0	1635	167.0
I-80	25.7	15300	16190	6.9500	196.0	1645	167.9
	D_p = 0.7986 cm, A_p = 2.002 cm², V_p = 0.1734 cm³, D_c = 2.35 cm, D_p/D_c = 0.3398, C_f = 1.048						
I-82	28.9	567.5	595.0	0.8243	21.41	161.5	17.05
I-83	29.4	861.8	903.0	1.0079	25.83	191.0	20.27
I-85	28.4	1406	1472	1.3197	35.01	269.0	27.01
I-86	28.6	1693	1975	1.4841	39.04	297.0	31.32
I-88	27.5	2205	2310	1.5902	43.33	344.0	35.83
I-90	26.4	2694	2825	1.7339	48.71	403.0	41.52
I-91	25.2	3930	4120	2.3979	69.00	592.0	59.98
I-92	25.0	5210	5460	2.8475	82.30	710.0	71.73

Table II. Continued

Run no. 1	T, °C 2	N_{Re} 3	N_{Rec} 4	$N \times 10^5$, g/cm²-s 5	$k_c^* \times 10^4$, cm/sec 6	N_{Sh} 7	$N_{Sh}N_{Sc}^{-1/3}$ 8
	D_p = 0.7986 cm, A_p = 2.002 cm², V_p = 0.1734 cm³, D_c = 2.35 cm, D_p/D_c = 0.3398, C_f = 1.048						
I-93	24.9	6480	6800	3.4053	98.60	856.0	86.34
I-94	25.1	7800	8175	4.0356	116.2	1002	101.4
I-95	25.2	9150	9600	4.2004	120.8	1040	105.4
I-96	25.1	10450	10950	4.7833	135.5	1170	118.4
I-97	24.9	11700	12270	5.2454	151.8	1318	132.9
I-98	24.6	12790	13400	5.3578	156.8	1420	142.7
I-99	25.3	14450	15150	6.2570	179.0	1530	154.0
I-100	23.4	14750	15580	5.9656	181.5	1758	173.2
	D_p = 0.5961 cm, A_p = 1.115 cm², V_p = 0.090 cm³, D_c = 2.35 cm, D_p/D_c = 0.2537, C_f = 1.040						
I-101	26.5	204.0	212.0	0.7026	19.28	118.5	12.22
I-102	27.3	1022	1062	1.5135	40.30	240.5	25.00
I-103	27.8	1241	1291	1.6555	43.50	254.0	26.56
I-108	28.3	1680	1748	1.8281	47.30	273.8	28.77
I-109	28.3	1890	1965	2.1562	55.70	322.5	33.89
I-110	25.8	2995	3115	2.5636	72.20	450.0	45.97
I-112	25.9	3970	4125	3.0868	86.50	540.0	55.20
I-113	26.0	4970	5170	3.8566	107.8	670.0	68.64
I-114	26.1	5970	6220	4.4844	124.8	776.0	79.57
I-118	26.4	10050	10450	5.9344	163.0	1002	102.9
I-125	26.1	11480	10900	6.3006	175.0	1098	111.9
	D_p = 1.138 cm, A_p = 4.080 cm², V_p = 0.4835 cm³, D_c = 2.97 cm, D_p/D_c = 0.3831, C_f = 1.058						
II-1	31.6	264.0	279.0	0.5672	13.00	145.0	15.90
II-2	31.5	529.0	560.0	0.5849	13.5	146.4	16.20
II-3	31.4	792.0	838.0	0.5971	13.9	157.0	17.10
II-4	31.4	1060	1121	0.7645	18.2	205.0	22.44
II-6	31.4	1320	1396	0.7855	18.7	211.0	23.00
II-9	31.4	1850	1957	1.0936	26.1	294.0	32.00
II-12	31.4	2110	2232	1.1612	27.7	312.0	34.00
II-15	31.4	2372	2509	1.2977	31.0	349.0	38.00
II-17	24.9	6681	7067	2.5852	76.9	1042	102.0
II-20	26.2	11300	11952	4.1620	119.3	1525	153.7
	D_p = 1.138 cm, A_p = 4.080 cm², V_p = 0.4835 cm³, D_c = 5.71 cm, D_p/D_c = 0.1993, C_f = 1.015						
III-1	16.2	53.00	53.80	0.1605	6.300	112.0	9.00
III-2	16.3	102.0	103.5	0.1795	7.010	124.1	10.1
III-3	16.8	152.0	154.0	0.2230	8.600	149.0	12.0
III-4	17.9	212.0	215.0	0.2503	9.310	156.0	13.0
III-8	21.0	400.0	406.0	0.3774	12.70	190.0	17.0
III-12	21.0	513.0	521.0	0.4631	15.60	234.0	21.0
III-13	21.2	573.0	582.0	0.4774	15.90	238.0	22.0
III-14	21.3	1150.0	1167	0.6856	22.20	329.0	30.0

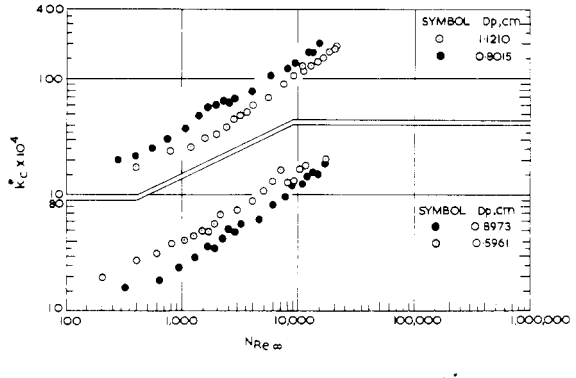

Figure 2. Effect of particle size on k_c^*

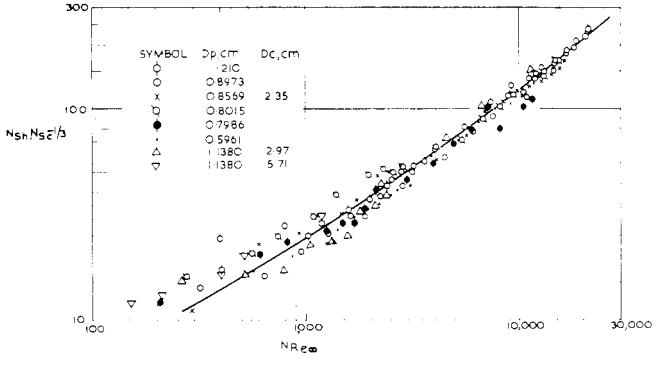

Figure 3. $N_{Sh}N_{Sc}^{-1/3}$ vs. $N_{Re\infty}$ plot for all runs

(*37*), on the other hand, have shown it to be a contribution of both molecular diffusion and natural convection and have found that

$$A = 2 + f(N_{Gr}N_{Sc}) \quad (6)$$

In all these correlations, no attention has been paid to the contribution from the wake of the sphere which becomes much appreciable at higher flow rates. Unfortunately, this is not amenable to rigorous theoretical treatment. Churchill and coworkers (*4, 43*) suggested that the contribution of the wake is directly proportional to the Reynolds number. The general equation for forced convective mass transfer from sphere then becomes

$$N_{Sh} = 2 + f(N_{Gr}N_{Sc}) + BN_{Re}^{1/2}N_{Sc}^{1/3} + CN_{Re}N_{Sc}^{1/3} \quad (7)$$

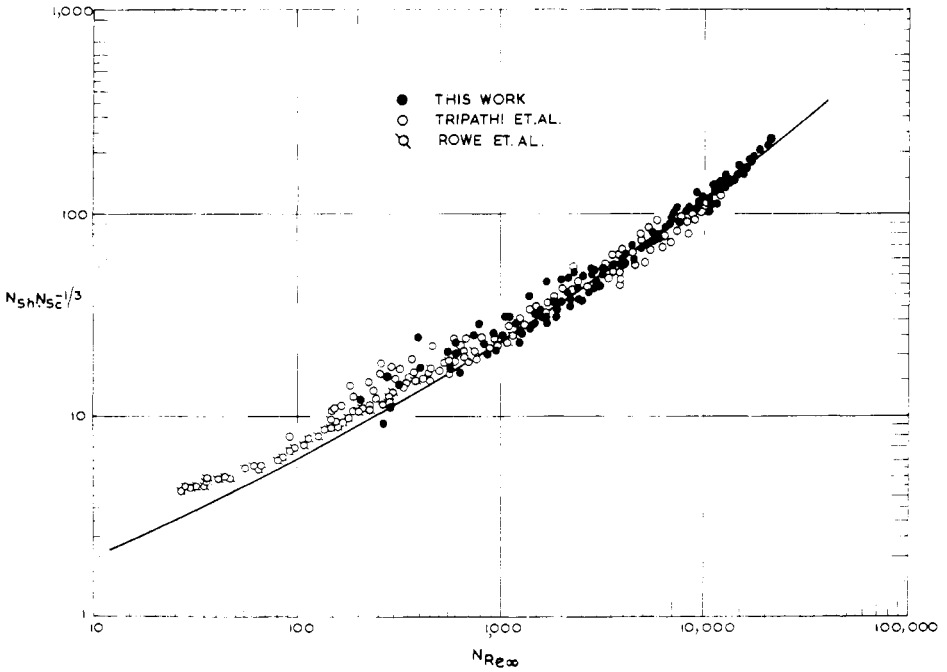

Figure 4. $N_{Sh}N_{Sc}^{-1/3}$ vs. $N_{Re\infty}$ plot: comparison with data for spheres

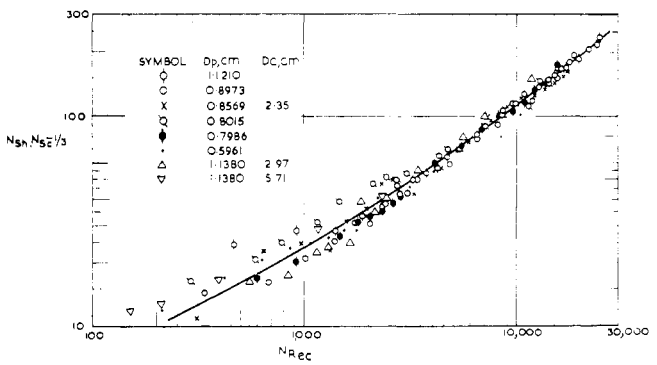

Figure 5. $N_{Sh}N_{Sc}^{-1/3}$ vs. N_{Rec} plot for all runs

This form has been successfully used by Kinnard et al. (*22*) for correlating the forced convective mass transfer data for spheres. The direct proportionality between wake Sherwood number and Reynolds number has not been accepted by many, and equations are available where wake contribution uses lower Reynolds number exponents such as 0.78, 0.80, or 0.82 (*2, 24*).

An attempt has been made to correlate the present results in terms of Equation 7 after neglecting the molecular diffusion and natural convection terms because these are insignificant for higher Reynolds numbers. Thus, Equation 7 for the present case becomes

$$N_{Sh}N_{Sc}^{-1/3} = BN_{Re}^{1/2} + CN_{Re}^{m} \quad (8)$$

The values of coefficients B and C and exponent m have been decided by the iterative least-squares analysis. This gave

$$N_{Sh}N_{Sc}^{-1/3} = 0.5854\ N_{Re\infty}^{1/2} + 0.005259\ N_{Re\infty} \quad (9)$$

and

$$N_{Sh}N_{Sc}^{-1/3} = 0.5844\ N_{Rec}^{1/2} + 0.006012\ N_{Rec} \quad (10)$$

which correlated the present data with average deviations of ±10.54 and ±9.58%, respectively. Use of exponents 0.78, 0.8, and 0.82 in place of 1 gave higher deviations. The validity of Equations 9 and 10 is clearer from Figures 7 and 8, which show the plots of $N_{Sh}N_{Sc}^{-1/3}N_{Re\infty}^{-1/2}$ vs. $N_{Re\infty}^{1/2}$ and $N_{Sh}N_{Sc}^{-1/3}N_{Rec}^{-1/2}$ vs. $N_{Rec}^{1/2}$, respectively, which are straight lines as expected; it is further evident that these equations can successfully correlate the data of Tripathi et al. (*40*) for spheres. The data of Rowe et al. (*31*) in the higher N_{Re} range are also in close agreement, but the data in the lower range are slightly higher.

Conclusions

The mass transfer coefficient increases with decreasing particle size. The effect of particle-to-column diameter ratio is absent up to $D_p/D_c = 0.477$. The mass transfer data for small nonspherical particles can be correlated by $N_{Sh}N_{Sc}^{-1/3} = 0.5844\ N_{Rec}^{1/2} + 0.006012\ N_{Rec}$, considering the contributions from both forward and wake portions.

Nomenclature

A = constant
A_p = surface area of a pellet, L^2
B = constant
C = constant
C_b = bulk concentration, M/L^3
C_f = blockage ratio, $u_c/u_\infty = 1/[1 - 2/3\ (d_s/D_c)^2]$
C_s = saturation concentration, M/L^3
d_s = diameter of the sphere, L
D = characteristic dimension parameter, L
D_c = column diameter, L
D_p = equivalent particle diameter, L
D_v = diffusion coefficient, L^2/t
f = a function
g = acceleration due to gravity, L/t^2
m = a constant
N_{Gr} = Grashof number = $(D^3g/\nu^2 \cdot \Delta\rho/\rho)$
k_c = mass transfer coefficient, L/t
N_{Re} = Reynolds number = $(Du\rho/\mu)$

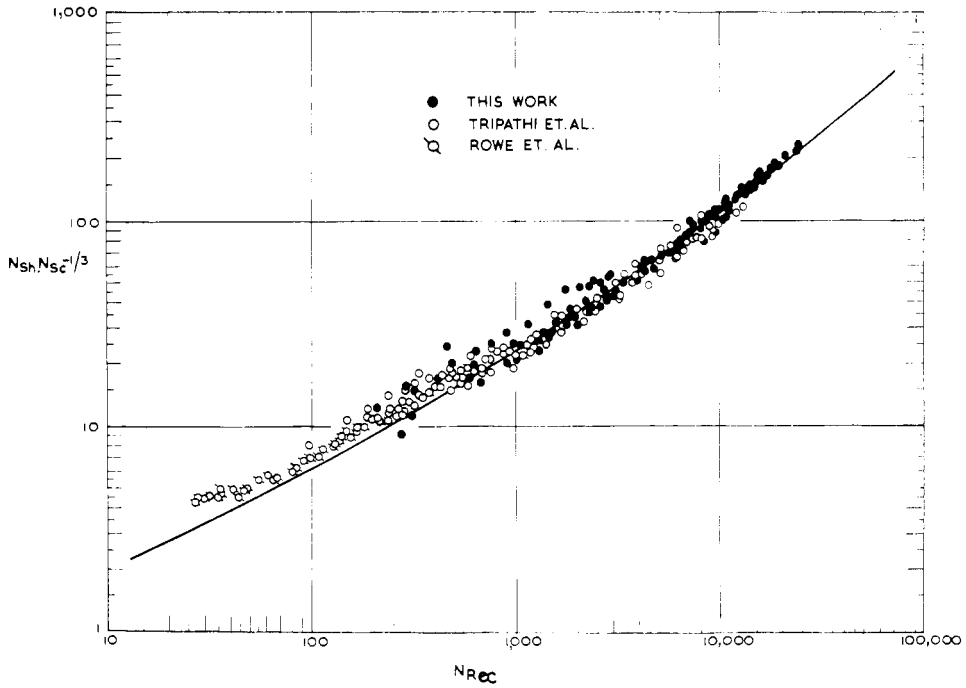

Figure 6. $N_{Sh}N_{Sc}^{-1/3}$ vs. N_{Rec} plot: comparison with data for spheres

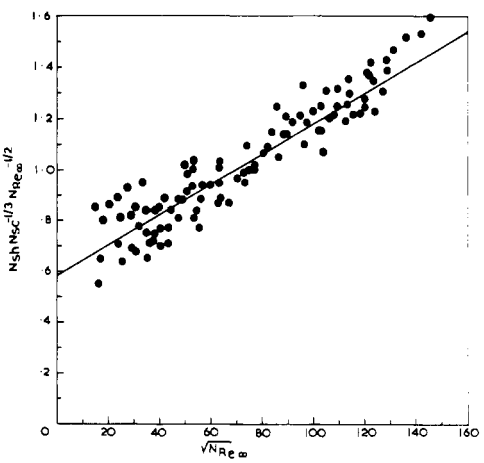

Figure 7. $N_{Sh}N_{Sc}^{-1/3}N_{Re\infty}^{-1/2}$ vs. $\sqrt{N_{Re\infty}}$ plot

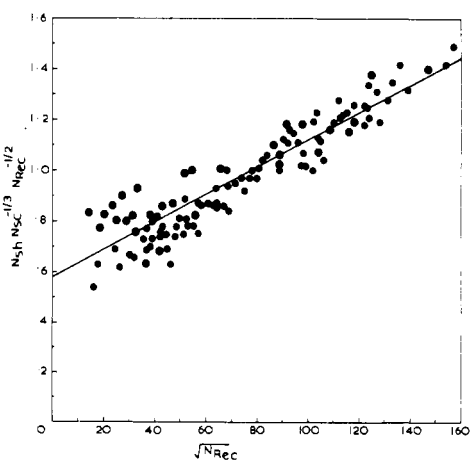

Figure 8. $N_{Sh}N_{Sc}^{-1/3}N_{Rec}^{-1/2}$ vs. $\sqrt{N_{Rec}}$ plot

N_{Rec} = particle Reynolds number = $(D_p u_c \rho/\mu)$
$N_{Re\infty}$ = particle Reynolds number = $(D_p u_\infty \rho/\mu)$
N_{Sc} = Schmidt number = $(\mu/\rho D_v)$
N_{Sh} = Sherwood number = $(k_c^{\cdot} D/D_v)$ or $(k_c^{\cdot} D_p/D_v)$
t = time of run, t
u = flow velocity, L/t
u_c = corrected flow velocity, L/t
u_∞ = free stream flow velocity, L/t
ΔW = weight loss during a run, M

Greek Letters

μ = viscosity, M/Lt
ν = kinematic viscosity = (μ/ρ), L^2/t
ρ = density, M/L^3
$\Delta\rho$ = density difference, M/L^3

Literature Cited

(1) Brown, N. S., Pitts, C. C., Leppert, G., *J. Heat Transfer*, **84,** 133 (1962).
(2) Chukhanov, Z. F., *Int. J. Heat Mass Transfer*, **14,** 337 (1971).
(3) Colburn, A. P., *Trans. Am. Inst. Chem. Eng.*, **29,** 174 (1933).
(4) Douglas, W.J.M., Churchill, S. W., *Chem. Eng. Prog. Symp. Ser. No. 18*, **52,** 23 (1956).
(5) Eisenberg, M., Chang, P., Tobias, C. W., Wilke, C. R., *Am. Inst. Chem. Eng. J.*, **1,** 552 (1955).
(6) Fröessling, N., *Beitr. Geophys.*, **51,** 67 (1937).
(7) Fröessling, N., *ibid.*, **52,** 170 (1938).
(8) Fröessling, N., *Lunds. Univ. Arsskr, N.F.*, **36** (4) (1960).
(9) Fuch, N. A., "Evaporation and Droplet Growth in Gaseous Media", Pergamon Press, London, England, 1959.
(10) Galloway, T. R., Sage, B. H., Document 9428, Am. Doc. Inst., Washington, D.C., 1967.
(11) Galloway, T. R., Sage, B. H., *Int. J. Heat Mass Transfer*, **10,** 1195 (1967).
(12) Garner, F. H., Grafton, R. W., *Proc. Roy. Soc.*, **A224,** 64 (1954).
(13) Garner, F. H., Keey, R. B., *Chem. Eng. Sci.*, **9,** 119 (1958).
(14) Garner, F. H., Suckling, R. D., *AIChE J.*, **41,** 114 (1962).
(15) Gibert, H., Couderc, J. P., Angelino, H., *Chem. Eng. Sci.*, **27,** 45 (1972).
(16) Grafton, R. W., *ibid.*, **18,** 457 (1963).
(17) Griffith, R. M., *ibid.*, **12,** 198 (1960).
(18) Harriot, P., *Can. J. Chem. Eng.*, **40,** 60 (1962).
(19) Hsu, N. T., Sato, K., Sage, B. H., *Ind. Eng. Chem.*, **46,** 870 (1954).
(20) Kafarev, V. V., *Zh. Prikl. Khim.*, **33,** 1495 (1960).
(21) Keey, R. B., Glane, J. B., *Can. J. Chem. Eng.*, **42,** 227 (1964).
(22) Kinnard, G. E., Manning, F. S., Manning, W. P., *Brit. Chem. Eng.*, **8,** 320 (1963).
(23) Langmuir, I., *Phys. Rev.*, **12,** 368 (1918).

(24) Lee, K., Barrow, H., *Int. J. Heat Mass Transfer*, **11**, 1013 (1968).
(25) Maxwell, R. W., Storrow, J. A., *Chem. Eng. Sci.*, **6**, 204 (1957).
(26) Pei, D.C.T., *Int. J. Heat Mass Transfer*, **12**, 1707 (1969).
(27) Perry, J. H., "Chemical Engineer's Handbook", 4th ed., McGraw-Hill, New York, N.Y., 1963.
(28) Pope, A., "Wind Tunnel Testing", Wiley, New York, N.Y., 1954.
(29) Ranz, W. E., Marshall, W. R., *Chem. Eng. Prog.*, **48**, 141 (1952).
(30) Robinson, W., Han, L. S., Essig, R. H., Haddelson, C. F., Ohio State Univ. Research Found. Rept., 41, 1951.
(31) Rowe, P. N., Claxton, K. T., Lewis, J. B., *Trans. Inst. Chem. Eng.* (*London*), **43**, T14 (1965).
(32) Ruckenstein, E., *Chem. Eng. Sci.*, **18**, 233 (1963).
(33) Seidell, A., "Solubilities of Inorganic and Organic Compounds", 3rd ed., Von Nostrand, New York, N.Y., 1941.
(34) Seidell, A., Linke, W. F., "Solubilities of Inorganic and Organic Compounds", Supplement, 3rd ed., Van Nostrand, New York, N.Y., 1952.
(35) Skelland, A.H.P., "Diffusional Mass Transfer", Wiley, New York, N.Y., 1974.
(36) Steele, L. R., Geankoplis, C. J., *AIChE J.*, **5**, 178 (1959).
(37) Steinberger, R. L., Treybal, R. E., *ibid.*, **6**, 227 (1960).
(38) Stephen, H., Stephen, T., "Solubilities of Inorganic and Organic Compounds", Pergamon Press, New York, N.Y., 1963.
(39) Topley, B., Whytlawgray, R., *Phil. Mag.*, **4**, 873 (1927).
(40) Tripathi, G., Singh, S. K., Upadhyay, S. N., *Ind. J. Technol.*, **9** (1971).
(41) Upadhyay, S. N., Tripathi, G., *J. Chem. Eng. Data*, **20**, 20 (1975).
(42) Vliet, G. C., Leppert, G., *J. Heat Transfer*, **83**, 163 (1961).
(43) White, R. R., Churchill, S. W., *AIChE J.*, **5**, 354 (1959).
(44) Wilke, C. R., Chang, P., *ibid.*, **1**, 264 (1955).

Received for review August 4, 1971. Resubmitted April 17, 1975. Accepted October 13, 1975.

Dielectric Constants, Viscosities, and Related Physical Properties of Several Substituted Liquid Ureas at Various Temperatures

Joseph Rosenfarb, Hugh L. Huffman, Jr.,[1] and Joseph A. Caruso*
Department of Chemistry, University of Cincinnati, Cincinnati, Ohio 45221

Dielectric constants, viscosities, densities, and refractive indices of three urea derivatives were measured at various temperatures ranging from 25 to 100 °C. The experimental data as functions of temperature were fitted precisely to appropriate equations. Dielectric constant data indicated a significant increase in dielectric constant of the cyclic ureas over that of the acyclic homologs. Kirkwood correlation factors and the activation energies of viscous flow were also evaluated. Values for Kirkwood correlation factors ranged from 1.07 to 1.21. This range indicates but does not substantiate parallel dipole association. Activation energies ranged from 3.3 to 4.4 kcal/mol.

Tetramethylurea (TMU) has been a very versatile solvent for a number of investigations (*2, 8, 14*); however, analogs such as tetraethylurea (TEU) and the substituted cyclic ureas (Figure 1) have not been so thoroughly investigated. Available physical data for these interesting compounds are limited even though they have been available for some time (*5, 24, 26, 28*). [The dielectric constant of TEU has been previously investigated by Beguin and Gäumann (*5*) over the temperature range −68 to 134 °C.] Their relatively high polarities, large liquid ranges, and slightly basic nature make these substituted ureas potentially useful dipolar aprotic solvents. Tetraethylurea, for example, has recently been successfully used as a solvent for electrical conductivity studies (*3*). Presently, in this laboratory, *N,N'*-dimethylethyleneurea (DMEU) and *N,N'*-dimethylpropylene urea (DMPU), shown in Figure 1, are also being investigated as electrolytic solvents. The cyclic ureas have larger polarities with dipole moments of 4.09 (*26*) and 4.23 (*26*) for DMEU and DMPU, respectively, as compared with 3.45 for acyclic TEU (*5*). In addition, their dielectric constants are at least twice as high as will be shown below.

[1] Present address, Exxon Research and Engineering Co., Box 121, Linden, N.J. 07036.

Experimental

Reagents. TEU was obtained from the RSA Corp. (Ardsley, N.Y.) and was purified by vacuum distillation as previously described (*8*). The specific conductance of TEU was 7.9×10^{-9} ohm^{-1} cm^{-1}. DMEU was synthesized by combining 2-imidazolidinone (Eastman), 80% formic acid (MCB reagent ACS), and 37% formaldehyde solution (Mallinkrodt Analytical reagent), in molar ratios of 5:50:8, respectively (*20*). Initially, the mixture warmed and the solution yellowed. Distinct color changes from yellow to orange, red, and finally brown were observed during the initial 8 h of the 48-h reflux period. Excess reagent solvents were removed under vacuum using a rotoevaporator; after the solution was made basic with saturated NaOH, the product was distilled at 65–72 °C (~2 mm Hg). Another distillation, over BaO at 65 °C (2 mm Hg), provided a colorless liquid in contrast to the yellow appearance of the crude distillate. Successive fractional freezings (*11*) then gave a very pure product with a specific conductance ranging from $1–7 \times 10^{-8}$ ohm^{-1} cm^{-1}. The liquid range for DMEU was determined as 8.2–220 °C (~754 mm Hg).

DMPU was prepared in a similar manner using 5 moles of 2-(1H)-tetrahydropyrimidinone (Eastman) in the starting mixture. No dramatic color change occurred as with DMEU, and the solution remained yellow. Fractional freezings were not practical due to the low freezing point (below −20 °C) of the substance. DMPU has a boiling point of 230 °C (~754 mm Hg). The pure distillate, distilled over BaO, had a specific conductance of 4.73×10^{-8} ohm^{-1} cm^{-1} and a boiling point of 81 °C (2.8 mm Hg). Boiling points agreed very well with literature data of 67 °C (2 mm Hg) (*26*), 84 °C (2 mm Hg) (*26*), and 30 °C (~2 mm Hg) (*3*) for DMEU, DMPU, and TEU, respectively.

Mass spectral, IR, and NMR data confirmed the DMEU and DMPU structures. The mass spectral data were gathered using a Hitachi Perkin-Elmer Model RMU-7 mass spectrometer. IR spectra were taken on a Perkin-Elmer 337 grating spectrometer and revealed virtually no OH stretch from 3350 to 3650 cm^{-1} when the solvent was transferred under anhydrous conditions to the cell. NMR spectra were taken using a